The development of a linear cutting machine used to characterize FEM modelling parameters for cutting UG2 Reef

by U. Du Preez[1], P.S.Heyns[1], and D.F. Malan[1]

Affiliation:
[1]University of Pretoria, South Africa

Correspondence to:
U. Du Preez

Email:
ulla.dup@gmail.com

Dates:
Received: May 2024
Revised: 28 Oct. 2024
Accepted: 29 Oct. 2024
Published: November 2024

How to cite:
Du Preez, U., Heyns, P.S. and Malan, D.F. 2024. The development of a linear cutting machine used to characterize FEM modelling parameters for cutting UG2 Reef. *Journal of the Southern African Institute of Mining and Metallurgy*, vol. 124, no.11 pp. 673–682

DOI:
http://dx.doi.org/10.17159/2411-9717/3394/2024

ORCiD:
P.S. Heyns
http://orcid.org/0000-0002-6164-9490
D.F. Malan
http://orcid.org/0000-0002-9861-8735

Abstract

South Africa has two main platinum reef deposits, namely the Merensky reef and the UG2 reef. These reefs are currently mined using traditional drilling and blasting methods. Mechanized cutting could potentially enable continuous mining, which would offer significant advantages. This would require thorough understanding of the cutability of the rock. To explore this, a linear cutting machine was developed to conduct laboratory scale cutting tests. This work describes the development and commissioning of the cutting machine using sandstone, as well as subsequent characterization tests on UG2 reef samples.

UG2 reef has large variability in strength on a millimeter scale. This introduces uncertainty in the test results due to added variance from one cut to the next for the same UG2 reef sample. Another problem is the variability in rock properties of the UG2 reef, when testing samples from different mines. The cutting tests led to fine fragmentation, which is known to be a significant problem for cleaning operations in underground stopes and warrants further research.

A finite element method simulation of the rock cutting was conducted using ANSYS LS-DYNA and the continuous surface cap model to simulate rock cutting in the UG2 reef. It was found that it is possible to use LS-DYNA with the continuous surface cap model to model rock cutting of UG2 reef and get acceptable results, but the user must calibrate the model parameters using the experimental results. Therefore, the model is only fit for one set of cutting parameters and further work is required to generalize results.

Keywords

conical pick, continuous surface cap model, finite element method, linear cutting machine, specific energy, UG2 reef

Introduction

Traditional mining methods, involving drilling and blasting, have steadily been replaced by mechanized mining methods, to the extent that mechanized mining has become the predominant mode of mining for new mine developments in softer rock (Moxham, 2004). This is, however, not the case for gold mines, platinum mines and other hard rock mining operations in the South African Bushveld Complex.

South African gold and platinum mines have narrow tabular reefs, typically less than 1 m in height (Pickering, 2007). Equipment currently used for mechanized mining in soft rock are not suitable for narrow reef hard rock environments. The traditional drilling and blasting mining process is cyclic in nature. This constrains the rate of face advance and leads to poor utilization of the invested capital (Moxham, 2004).

Mechanized cutting offers the potential for continuous mining, which may lead to significantly improved rates of face advance (Vogt, 2016). Mechanized cutting does not cause instability of the rock due to explosions, there is no need to ventilate toxic gases before people can access the mine again after blasting, and it has the potential to reduce waste dilution (Moxham, 2004; Pickering, 2007). The cutting characteristics of South African hard rock narrow reef environments are not well understood, and this impedes the introduction of mechanical rock cutting in these mines.

Various researchers have used linear cutting machines (LCMs) to conduct laboratory scale cutting tests on different rock samples, using different cutting methods (Bilgin, et al., 2013; Copur, et al., 2017; Dehkhoda and Detournay, 2019; Hekimoglu, 2018; Kang, et al., 2016; Li, et al., 2022; Mendyka, 2017; Park, et al., 2018). In these tests, the cutting parameters were changed to determine the effect on the performance of the cutting method for a specific rock sample. Most of these tests were conducted using artificial rock samples, such as cement mortars and sandstones. There is, however, a dearth of research on South African hard rock types, such as UG2 reef.

Cutting parameters and cutting forces determined from laboratory scale experiments can be used to numerically simulate rock cutting using the finite-element method (FEM) (Huang, et al., 2016; Jaime, et al., 2015; Wicaksana, et al., 2021). Most of the numerical modelling for rock cutting are either for conical picks or symmetrical disk cutting used by tunnel boring machines (TBMs) (Stopka, 2021). The level of complexity of numerically modelling rock cutting using FEM is based on the selection of an appropriate rock failure model. The basic model frequently used is the Mohr-Coulomb failure criterion, whereas more advanced models include the concrete damage model, the Johnson Holmquist concrete model, and the continuous surface cap model (CSCM). Jaime (2015) compared these more advanced models and found that the CSCM gives the most realistic cutting forces and fragmentation patterns (Jaime, et al., 2015). This model was therefore used in this study.

Huang et al. (2016) used FEM for modelling of rock cutting using a conical pick. They compared the mean cutting forces and the peak cutting forces obtained from the simulation to theoretical values that were determined by using the equations given by Evans (1962) and Goktan (1997), as well as experimental values. The numerical simulations showed that there are various model parameters that influence the results and others have little effect. Previous research showed that there are many choices that need to be made about model parameters, such as element size, element type, boundary conditions, contact parameters and model parameters. Some are based on material properties and other are obtained through trial and error.

This work describes the development of a linear cutting machine (LCM) to determine the cutability of UG2 on laboratory scale samples. The first part of the work describes the development of the LCM, which was commissioned using sandstone with little to no variance in strength on a millimeter scale. Once the LCM was commissioned, various laboratory scale cutting tests with different cutting parameters were conducted on UG2 samples. The objective was to determine the impact of the different cutting parameters, to determine rock characteristics, and to investigate if the results follow the same trends as for other rock types. These UG2 rock characteristics are currently not available and represent an important new contribution.

The experimental results were used to calibrate the continuous surface cap model (CSCM) parameters, for one set of cutting parameters. The CSCM was selected because it was found by previous researchers to give good results for simulating rock cutting (Jaime, 2011; Huang, et al., 2016). The FEM results showed that it is possible to model rock cutting of UG2 reef using conical pick. The present model requires calibration of the model using a specific set of cutting parameters and experimental results. Further work is required to ensure applicability of the model over a range of cutting conditions.

Development of a linear cutting machine for the UG2 experiments

A linear rock cutting machine was developed for this investigation. This LCM had to meet various design requirements. The LCM had to be sufficiently robust and stable when subjected to the cutting forces experienced along all three orthogonal directions (Kang, et al., 2016). Additionally, it had to allow linear motion of the conical pick, thus simulating the cutting process. This could be accomplished by either pushing the rock or pushing the conical pick (Bilgin, et al., 2013; Copur, et al., 2017; Park, et al., 2018). Furthermore, the machine required the capability to measure three orthogonal cutting forces, namely drag force, normal force, and side force, as shown in Figure 1. Using the drag force, density, distance cut and mass of cut material, the specific energy could be determined for each cut. The specific energy is the amount of energy required to cut one cubic meter of material. The LCM should allow for accurate adjustments of the depth of cut, attack angle, skew angle, and cut spacing, as shown in Figure 1.

Linear cutting machine configuration

For this study, a radial arm drilling machine was modified to provide the translational degree-of-freedom requirements of the LCM. Figure 2 shows the different components of the LCM and the associated degrees-of-freedom.

A linear actuator moves horizontally, as shown by the red arrow. This horizontal movement simulates the cutting motion by pressing the pick through the rock. The linear actuator has a maximum horizontal movement of 240 mm. The speed at which it cuts can be adjusted. The radial arm drilling machine table allows for both horizontal and vertical movement. The vertical movement is shown by the yellow arrows. The table allows the cross-sliding table to move horizontally, as shown by the magenta arrow. Both the horizontal and vertical movement are used to move the rock specimen into the correct position. The cross-sliding table allows for accurate changes in cut spacing, shown by the light blue arrow. The spindle can move vertically, which allows for accurate changes to the cutting depth, shown by the green arrow. There are slots in the lower flange of the load cell assembly, which allow for change in the skew angle. The skew angle can be adjusted to a maximum of 30°. The attack angle can be changed by changing the bottom flange and pick holder. The bucket can hold a rock specimen with maximum dimensions of 500 mm wide, 250 mm long and 200 mm high. The bucket has a clamp that holds the rock specimen in place. The base

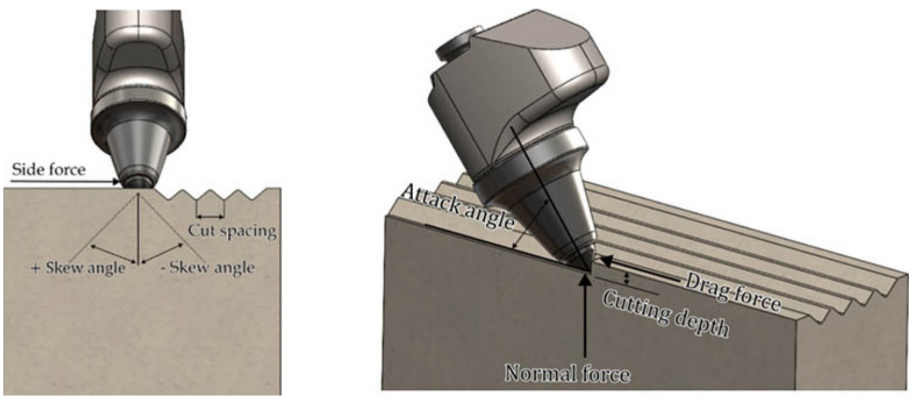

Figure 1—Degrees of freedom and cutting forces imposed by the LCM

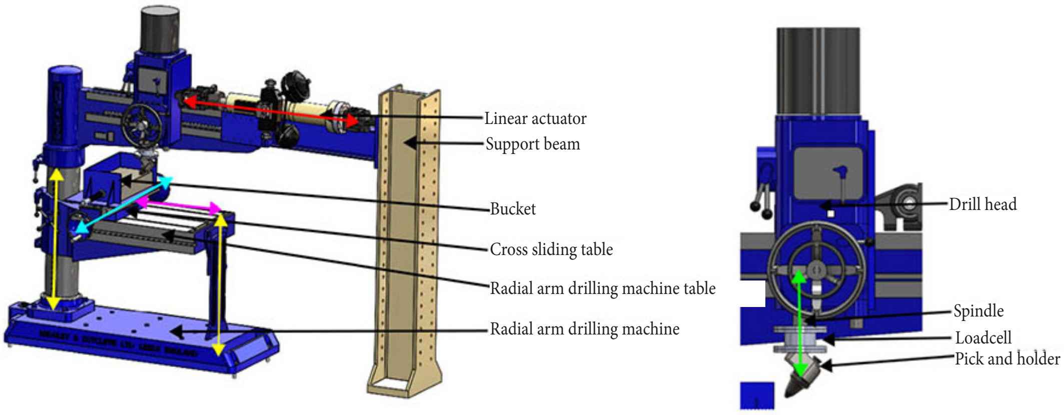

Figure 2—Degrees of freedom of the LCM

of the LCM is bolted to the ground. Because the LCM works as a press, all the forces act on the machine and not on the base. The base only gives stability. Figure 3 illustrates the dimensions of the conical pick used in the laboratory scale cutting tests.

A load cell was required to measure the cutting forces. This load cell was constructed by cementing four strain gauges to a cylindrical tube, as shown in Figure 4, and was calibrated by measuring strain while applying known forces. A combination of orthogonal forces was applied to emulate conditions during actual rock cutting.

The application of a combination of orthogonal forces for calibration purposes was done by pressing the point of the conical pick with a hydraulic jack and measuring the applied force. Two different combinations of forces were applied. The first was a combination of drag force and normal force, and the second was normal force and side force. The load cell outputs four values as measured by the half bridge strain gauges. These values were used in the linear equations as shown in Equations [1] to [3].

$$F_{Normal} = A_1\left(A_2SG_1 + A_3SG_3 + 2(A_4SG_2 + A_5SG_4)\right) \quad [1]$$

$$F_{Drag} = A_6\left(A_7SG_1 + A_8SG_3 + 2(A_9SG_2 + A_{10}SG_4)\right) \quad [2]$$

$$F_{Side} = A_{11}(A_{12}SG_4 - A_{13}SG_2) \quad [3]$$

where F_{Normal} is the predicted normal force, F_{Drag} is the predicted drag force, F_{Side} is the predicted side force, and SG_1 to SG_4 are the four strain gauge values. SG_1 is the value of the front strain gauge, which is in line with the cutting direction, as shown in Figure 4. The rest of the strain gauges are numbered anti-clockwize when looking from the top of the load cell.

A_1 to A_{13} are coefficients that were determined by minimizing the mean squared error for the calibration data. For the minimizing, Python scipy.optimize.minimize was used with the Broyden–Fletcher–Goldfarb–Shanno (BFGS) method. Table I shows the mean and standard deviation (std) of the absolute error of predicted values to actual values of the applied force.

Experimental set-up

For commissioning of the LCM, various cutting tests were conducted with different parameters on the sandstone sample. The drag force, normal force, and the side force, as shown in Figure 1, were measured for each cut and the cut material was gathered. The tests were performed at cutting depths of 2 mm and 4 mm. The cut spacing was changed so that the cut spacing to cutting depth ratio, s/d, was 1, 2, 3, 4, 5, and 6. The skew angle was changed from -10°, 0°, and 10°. The attack angle was kept constant at 50°. The cutting speed was the same for all the tests at 50 mm/s and a sampling rate of 300 Hz was used for strain gauge measurements on all the tests.

A cutting sequence comprized of firstly pre-cutting the surface to simulate a rock face (Park et al., 2018) and then nineteen subsequent cuts. The first cut was an initial cut. Then three of each cut spacing to cutting depth, s/d, ratios were cut. After each cut the cut material was collected and weighed. The weighed mass and the density of the material were used to determine the specific energy.

Figure 5 shows the cutting sequence for a cutting depth of 2 mm. In the cutting sequence the single black line at the bottom of the figure is the initial cut, the magenta represents the first three cuts at a cut spacing of 2 mm, the cyan lines are at a cut spacing of

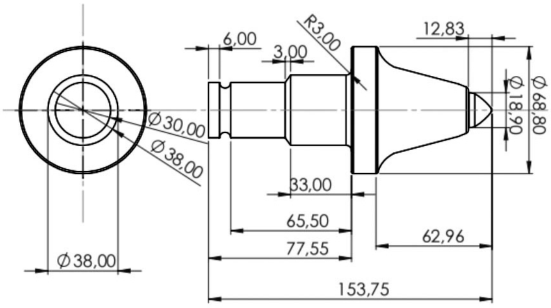

Figure 3—Conical pick dimensions

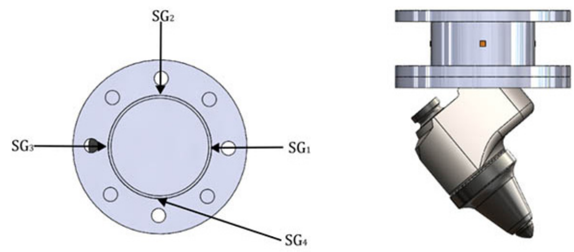

Figure 4—Strain gauge positions and load cell assembly

Table I

Absolute error of predicted values to actual values of the load cell

	Normal force [kN]	Drag force [kN]	Side force [kN]
Mean	0.0354	0.0179	0.0257
Std	0.0282	0.0235	0.0189

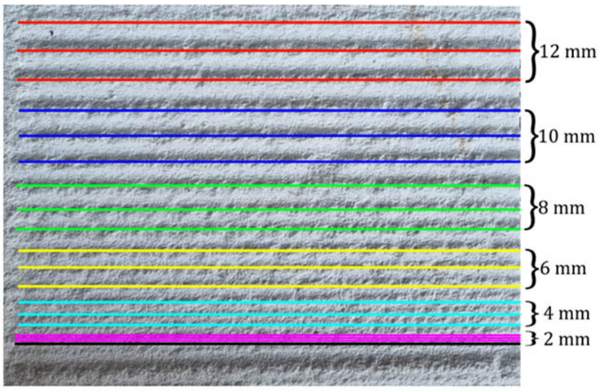

Figure 5—Cutting sequence at 2 mm cutting depth

4 mm, the yellow lines are at a cut spacing of 6 mm, the green lines are at a cut spacing of 8 mm, the blue lines are at a cut spacing of 10 mm, and the three red lines at the top of the figure are at a cut spacing of 12 mm. This is a total of 19 cuts.

The sandstone used for the commissioning had little to no variability in strength on a millimeter scale and was locally sourced from a building materials supplier. For the commissioning of the LCM, detailed measurements were obtained of the mean and peak drag force, normal force, and side force, as well as the specific energy for the different cut spacing to cutting depth ratios, s/d. These results were compared to results reported by Park et al. (2018). The results showed similarities in terms of magnitude of force values and the trends that occurred as the s/d ratio increased. For all the skew angles, the magnitude of the force increased linearly with the increase in s/d ratio. The negative skew angle experienced a higher magnitude in force at the same cutting depth and cut spacing and is similar to observations by Park et al. (2018). The specific energy had an optimum s/d ratio between 3 and 4.

A colour map was made of the mean force for all 19 cuts to show the variance in strength on a millimeter scale. Figure 6 illustrates one of these colour maps, where the map represents the surface of the sample as shown in Figure 5, and the x-axis is the cutting distance. The colour map shows how the cutting forces change as the s/d ratio changes and where more force was required to make a cut on the surface of the rock sample. The cutting distance is 150 mm. The cut is from left to right. The s/d ratio of one either starts at the top or at the bottom, depending on the direction of the cut sequence. To map the force the data of the 150 mm is divided into 12 sections. The mean of each section is then mapped. The mapping uses a bi-linear interpolation between runs. The following cutting parameter was used: a cutting depth of 2 mm with skew angle 0°. Figure 6 shows the drag force map for cutting sandstone at 2 mm cutting depth.

Figure 6 shows that the color remains fairly consistent for each run. Thus, showing the little to no variability in strength on a millimeter scale of the sandstone. The figure also shows how the mean drag force increases from run 2 to run 19, from bottom to top. For the first 10 mm of the cut the mean drag force is low, which is due to the cut initiation.

Results and discussion of experimentally cutting UG2

The previous sections demonstrate the use and some results that were obtained during the commissioning of the LCM. From these results it was concluded that the LCM was suitable to continue with the characterization tests on the UG2 reef samples. The following sections present detailed results obtained from cutting UG2 reef rock samples.

For this study, a UG2 reef sample was obtained from the Siyanda Bakgatla Platinum Mine, located at Swartklip, in Limpopo, South Africa. The rock sample was taken out of the underground mine and brought to the University of Pretoria laboratories. The sample was not affected by weathering. The sample was subsequently cut into manageable sized samples that were used in the laboratory scale cutting tests.

Laboratory scale cutting test results

The cutting sequence and method shown in Figure 5, was again used for cutting UG2 reef samples. The results of the laboratory scale cutting tests show the mean cutting forces, peak cutting forces, and the specific energy versus the cut spacing to cutting depth ratio, s/d. The cut spacing to cutting depth ratio was used to represent the data, because it is a dimensionless quantity. Thus, different cutting depths can be compared to one another (Park, et al., 2018). The graphs show the average value as well as the maximum and minimum values. This demonstrates the uncertainty in the data.

Effect of cutting parameters on drag force and normal force

Figure 7 to Figure 15 show the results obtained when cutting UG2 samples with the different cutting parameters. For a cutting depth of 2 mm both the mean normal force and mean drag force follow the same trend, where the mean force increases linearly with the cut spacing to cutting depth ratio, s/d. Also, the mean forces for a negative skew angle are higher than that of zero skew angle and

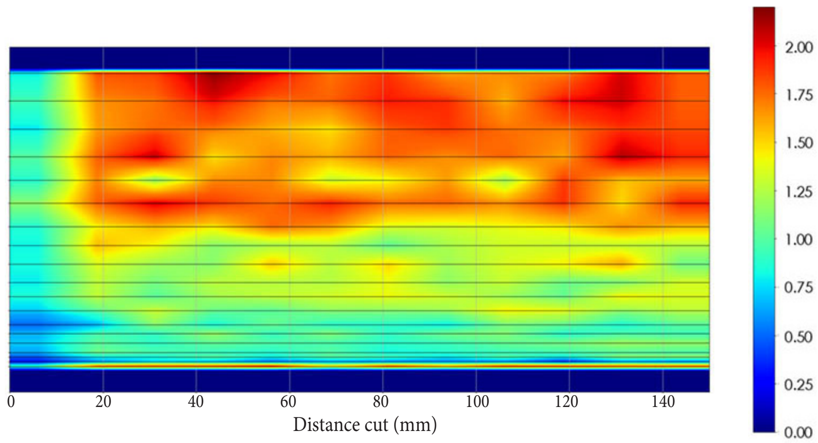

Figure 6—Drag force mapping of sandstone at skew angle = 0°

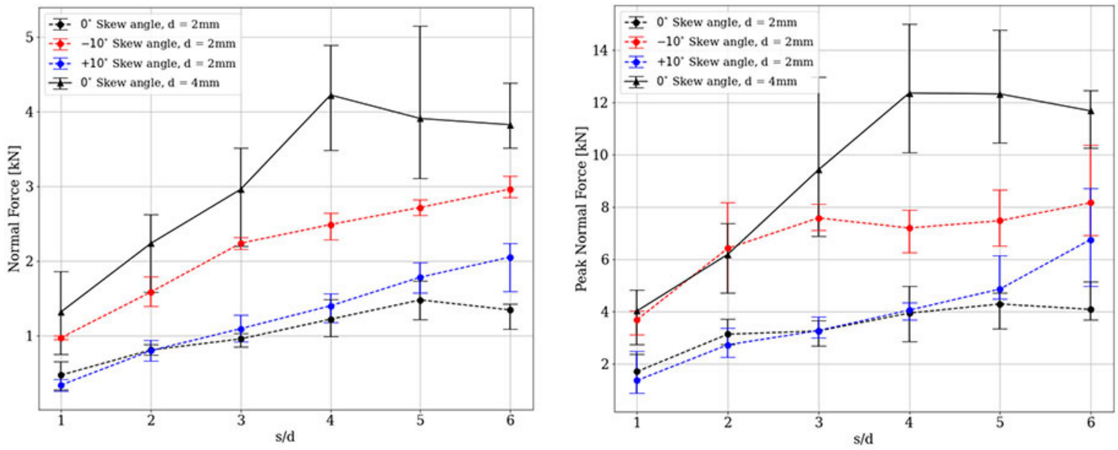

(a) Mean normal force *(b) Peak normal force*

Figure 7—Normal force cutting UG2

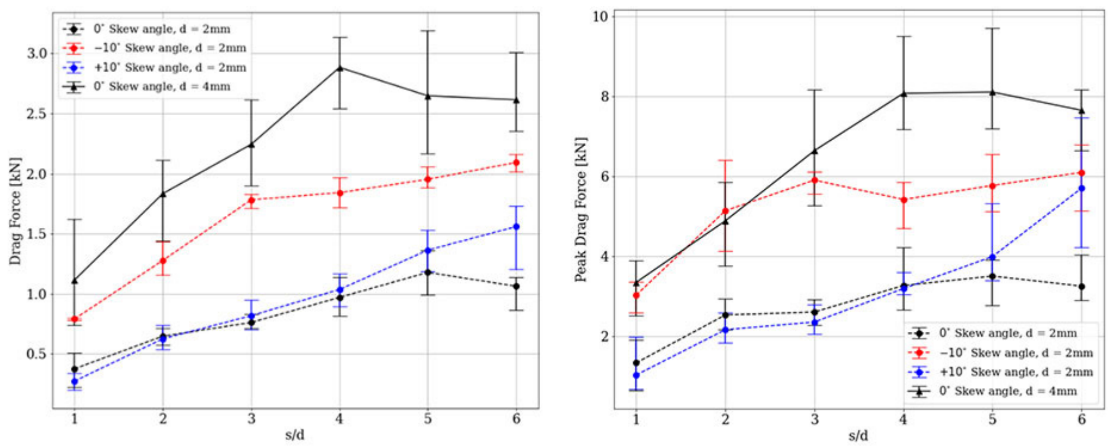

(a) Mean drag force *(b) Peak drag force*

Figure 8—Drag force cutting UG2

positive skew angle. The mean forces for zero skew angle and positive skew angle are similar to one another. The increase in force for negative skew angle is due to increase in contact area when a negative skew angle is applied.

The peak normal force and peak drag force follow a different trend than expected when compared with findings from previous researchers (Kang, et al., 2016; Park, et al., 2018). It was expected that, at all the skew angles, the peak forces increased linearly with the s/d. For the UG2 reef sample this linear relationship only occurred at a positive skew angle. For negative skew angle and zero skew angle, the peak forces level out at s/d values of 3 and 2, respectively. This is an interesting observation for the UG2 reef sample. This can be due to the large variability in strength on a millimeter scale in the rock sample, or due to the contact area between the pick and the UG2 at different skew angles, which will be discussed later.

For a cutting depth of 4 mm, both the mean normal force and mean drag force level out at an s/d of 4. This implies that at an s/d value of 4 and more, the previous cut does not have an influence on the next cut. Owing to this, increasing the s/d will not influence the cutting force results. This does not follow the same trend as the UG2 reef sample at 2 mm cutting depth. The plateaus show that the depth of cut has a larger influence on the cutting performance. This behaviour needs to be considered when designing cutting machines for deep hard rock environments.

Effect of cutting parameters on side force

When looking at the results of the side forces, it must be noted that at large s/d depth ratios the mean is close to zero. Thus, the maximum and minimum value will either be positive or negative and when examining the side force results, the magnitude is the important value and not the sign. Also, the sign of the side force is dependent on the direction of the cutting sequence. For positive and negative skew angles, the sign differs as expected because the cutting sequence is executed in different directions. Thus, the direction of the side force will differ. This is something that must be considered when examining the results of the side forces.

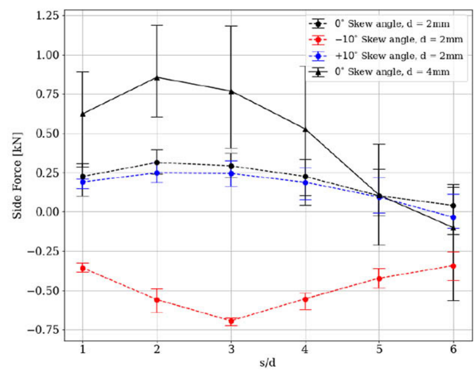

Figure 9—Mean side force cutting UG2

The skew angle influences the mean side force. For a negative skew angle, the magnitude in force values is the highest and a positive skew angle has the lowest magnitude in force values when compared at different s/d values. For the positive skew angle, the side force is close to zero at an s/d value of 5.

The reason is due to the change in the frontal area that is in contact with the rock when cutting. Figure 10 shows the frontal area when cutting an initial cut, with a skew angle of 10°. The yellow-coloured area on the left, represents the area of the pick where the rock will apply a force to the right on the pick. The area on the right (blue), represents the area of the pick where the rock will apply a force to the left on the pick. The grey area represents the rock that is being cut. The blue area is larger than the yellow area. Thus, the force to the left is larger for an initial cut.

For a small s/d cut with a positive skew angle there is only an area on the left (yellow), that will apply a force to the right on the pick. Thus, for the small s/d the force will be to the right. For a large s/d cut with a positive skew angle, there are both a yellow and a blue area, that have about the same area. Thus, the forces to the left and the right will cancel one another, and the force will be close to zero. For a small s/d cut with a negative skew angle there is only an area on the right (blue), where the rock will apply a force to the left on the pick. Thus, for the small s/d, the force will be to the left. For a large s/d cut with a negative skew angle there are both a yellow and a blue area, but the blue area is larger. Thus, the forces to the left are larger than the forces to the right, thus the force applied on the pick will be to the left.

Specific energy

The specific energy of the UG2 reef samples, at a cutting depth of 2 mm, follow the expected trend. When examining the optimal s/d value for the different skew angles, a higher s/d value of approximately 4 is optimal for a -10°. A lower s/d value is optimal for a skew angle of +10°. Thus, a value of either 2 or 3. For 0° skew angle a s/d value of either 3 or 4 will be optimal. One difference is that, for almost all the s/d values the specific energy is lower at a skew angle of 0° than a skew angle of +10°. This is not the same for material used by previous researchers (Kang, et al., 2016; Park, et al., 2018). The specific energy plateaus for a skew angle of 0° at an s/d value of 5. Figure 11 shows that there is a difference in the trend of the specific energy at different cutting depths. It was expected that the deeper the cut, the lower the specific energy for the different s/d values will be.

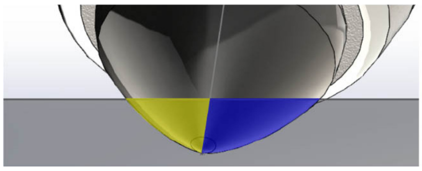

Figure 10—Frontal area for an initial cut with a skew angle

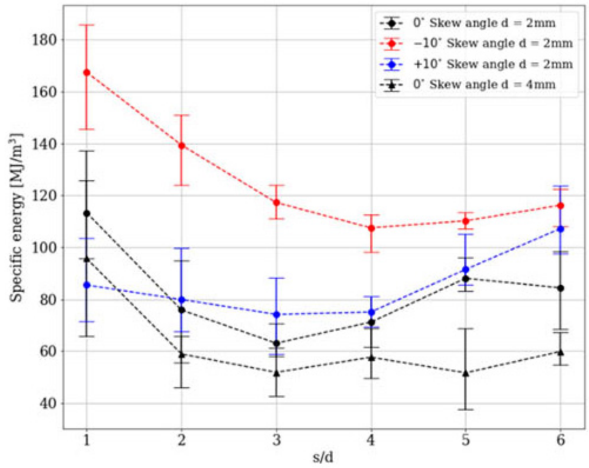

Figure 11—Specific energy cutting UG2

Both cutting depths show that an optimal s/d value is 3 when the skew angle is zero. At a cutting depth of 4 mm, the specific energy plateaus at an s/d of 4 when cutting UG2. This was the same for the normal forces and the drag forces. This implies that the deeper the cut the less influence the previous cut has at the same s/d.

Periodicity of the cutting force signals

Figure 12 and Figure 13 show the measured force signals at an s/d of 3, with cutting depths of 2 mm and 4 mm, respectively, when cutting UG2 reef samples. The skew angle is 0°.

The force signals are not regular in shape and amplitude, as shown in Figure 12 and Figure 13. In Figure 12 the amplitude is lower between a cutting distance of 60 mm to 80 mm. This shows inconsistency in strength of the sample being cut. A fast Fourier transform (FFT) analysis was done on the cutting force signals. The FFT showed that the drag force signal, when cutting UG2, is not periodic. This is consistent with the fact that UG2 does not display uniform chip formation. The fact that the UG2 has large variability in strength on a millimeter scale causes the cutting force to vary. Therefore, causing the cutting force to be non-periodic. Calculation

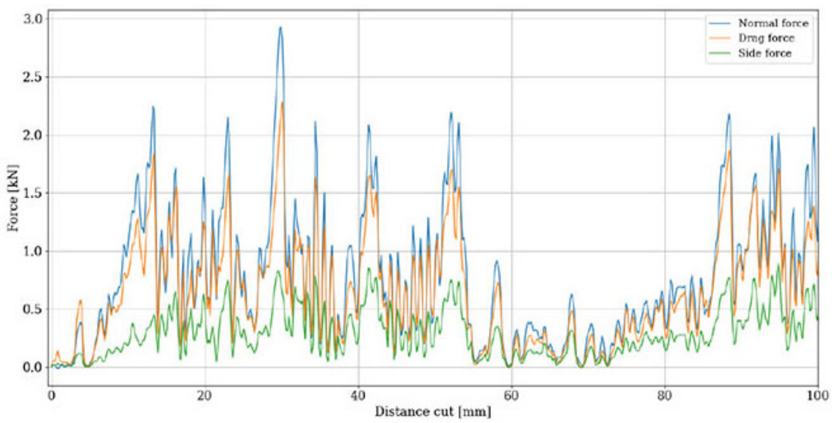

Figure 12—Cutting forces for UG2 rock sample at 2 mm cutting depth, s/d = 3 and skew angle = 0

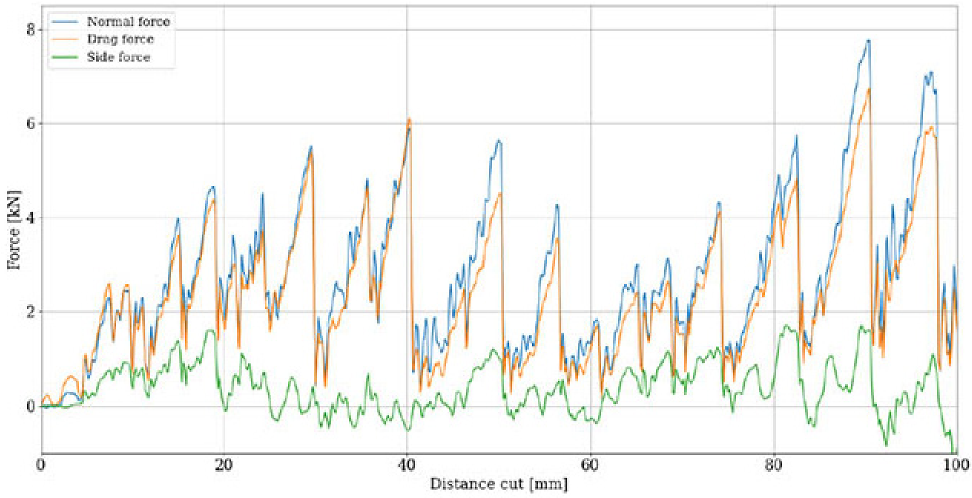

Figure 13—Cutting forces for UG2 rock sample at 4 mm cutting depth, s/d = 3 and skew angle = 0°

of the FFT confirms the observation that the chip forming is irregular. Figure 14 shows the cut material that was gathered for a 4 mm cutting depth. This fine material was also observed for a cutting depth of 2 mm.

The fine material shown in Figure 14 will be a significant problem for cleaning operations in underground stopes. Further work on this needs to be conducted and the reason for the fine fragmentation needs to be better understood.

Figure 14—Material gathered from cutting UG2

Rock homogeneity analysis

As discussed in the commissioning of the LCM, the variance in strength on a millimeter scale of the material can be revealed by plotting a colour map of the cutting forces. A similar approach was employed here to investigate the variance in strength on a millimeter scale of the UG2 reef samples. The plot, for the UG2 sample, was normalized by dividing the mean force of each section by the mean force of the run. This shows where in each run there were low and high forces, compared to the mean of the run. Figure 15 shows the normalized drag force map for cutting UG2 at a 2 mm cutting depth with skew angle 0°.

The normalized maps show that there is an inconsistency in the lower middle of the rock sample identified by the green box. This inconsistency was present in all three cutting sequences. It is assumed that the rock is weaker at this point, due to the lower force required to cut the rock. There are two other similar inconsistencies where it may be assumed that the rock is weaker. One is at the start of the cut, between 0 mm to 40 mm, shown by the orange box. The other is shown by the yellow box. The lower right corner is assumed to be stronger than the rest, due to the required force being higher than the mean, shown by the blue box. The normalized colour

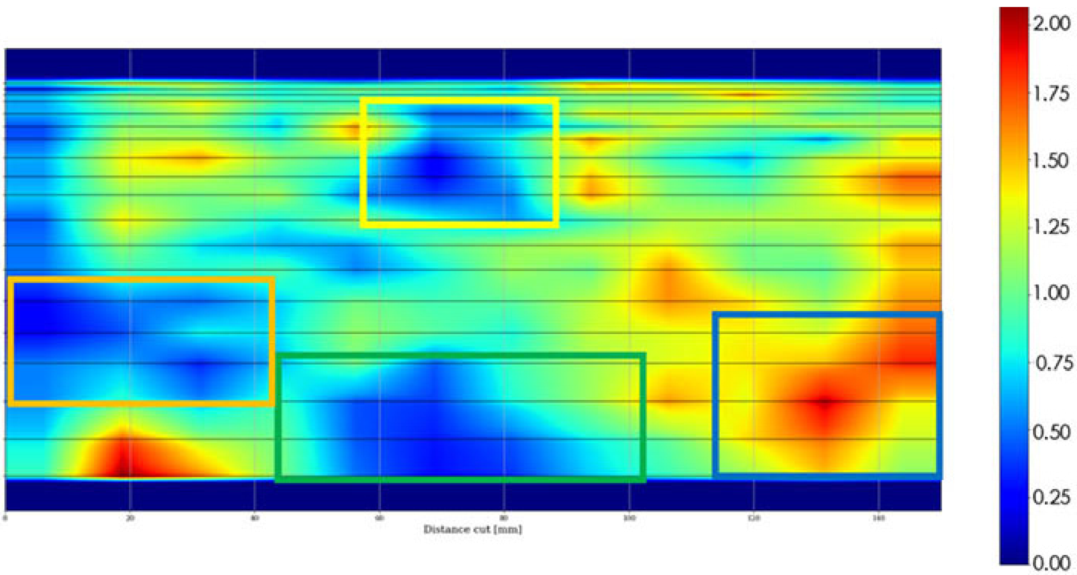

Figure 15—Normalized drag force mapping of UG2 at skew angle = 0°

maps clearly show that the UG2 rock sample has large variability in strength on a millimeter scale. One can expect that such a sample with large variability in strength on a millimeter scale will cause more variance in the cutting data. This can be seen in the cutting data shown in Figure 12.

Numerical simulation

Wider adoption of cutting solutions for the extraction of UG2 would require the ability to better simulate these cutting processes. This section discusses the numerical model developed for simulating rock cutting using conical picks. Ansys LS-DYNA was used for the modelling. As was motivated in the introduction, the continuous surface cap model (CSCM) was used as the failure model, because it allows for element erosion, which allows modelling of the fragmentation process. This model is typically not used in rock engineering studies and further work needs to be done to verify this model, and to determine the most applicable constitutive failure model for UG2 when mined using mechanical methods.

Finite element method set-up

There are various parameters that have to be selected and calibrated for the model. This includes mesh type, element size, contact properties, and boundary conditions. All these parameters have an influence on the computational time, efficiency, and simulation results.

A tetrahedron mesh was selected, following a recommendation by Jaime (2011) that a tetrahedron mesh gives a more realistic fracture pattern. Figure 16 illustrates the 3D view of the model set-up. An element size of 1.6 mm was used for the rock. The conical pick was modelled after the conical pick that was used in the experimental laboratory scale cutting tests. The pick has an element size of 1.2 mm. A vertex sizing with spherical influence at the tip of the pick was used, with a radius of 5 mm and an element size 0.4 mm. This ensures that the resolution of the pick shape at the tip is modelled accurately, but still saves computational time and resources. The pick is modelled as a rigid body.

For the numerical simulation, both side faces, the bottom face, and the back face were fixed. The front face, which will be in contact with the pick, was fixed in the z direction. For the ERODING_SURFACE_TO_SURFACE, a parameter of the LS-DYNA, all three parameters, the viscous damping coefficient, contact penalty scale factor, and the target penalty scale factor were selected as 5 (Livermore Software Technology (LST), an ANSYS company, 2021). The friction coefficient and the dynamic coefficient had an influence

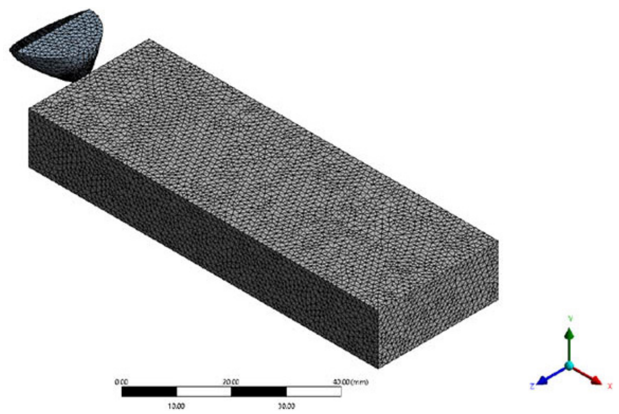

Figure 16—3D view of model set-up

on the ratio of normal force to drag force. Through trial and error, a friction coefficient of 0.004, a dynamic coefficient of 0.001, and a decay constant of 1 was used.

Höll (2009) reported data on the density, Young's modulus, and Poisson's ratio of UG2 from different areas in the South African Bushveld complex. This data was used as initial values of the rock properties to calibrate the CSCM. The parameters for the CSCM were updated by changing the material properties, used in the equations presented by Novozhilov et al. (2022). The parameters were selected to accurately predict the cutting forces at a cutting depth of 2 mm, then the same model with the same parameters were used at a cutting depth of 4 mm to determine if the model extrapolates accurately.

The Novozhilov et al. (2022) equations for the CSCM parameters require the specification of specific material properties. These properties were determined through trial and error. The specific material properties that were used are: Young's modulus 83.2 GPa, Poisson's ratio 0.152, density 4.19 g/cm^3, uniaxial compressive strength 70 MPa, and aggregate size 19 mm. These values of the material parameters fall in the range of values of UG2 reef samples. The aggregate size was chosen as the default value used by the CSCM. Determining the rock properties of UG2 reef rock is difficult due to the very large variability of this rock type. The only property that was known, of the sample that was used in the experimental cutting tests, is the density of the UG2 reef sample.

Numerical simulation results

In this section the numerical simulation results are compared to the experimental cutting results, when cutting UG2 samples, for the three initial cuts, no influence of previous cuts, at 2 mm cutting depth and 4 mm cutting depth with a skew angle of zero. Table II shows the data that was used to compare the experimental results to the numerical simulation results.

In this table FN is the normal force, FD is the drag force, FN' is the peak normal force and FD' is the peak drag force.

Table III shows the maximum error value and the maximum percentage error for the results of the experimental cutting forces compared to the mean of the three runs, at 2mm cutting depth.

Table IV and Table V show the results obtained for the numerical simulations at a cutting depth of 2 mm and 4 mm. The tables also show the percentage error between the numerical simulation results and the experimental results.

Table II

Experimental cutting data for UG2 at 2 mm and 4 mm cutting depth

Cutting depth	FN [kN]	FD [kN]	FN' [kN]	FN'/FN	FD'/FD	FN/FD
2 mm	1.25	1	3.83	3.064	3.15	1.25
4 mm	3.8	3.01	11.24	2.96	2.96	1.26

Table III

Maximum error for experimental runs at 2 mm cutting depth

	FN error	FD error	FN' error	FD' error
Value [kN]	0.2	0.16	0.2	0.24
%	16.32	15.52	5.21	7.54

Table IV
Numerical simulation force results for UG2 reef

Cutting depth	FN [kN]	% Error	FD [kN]	% Error	FN' [kN]	% Error	FD' kN]	% Error
2 mm	1.128	9.76	1.11	11.06	3.346	12.63	3.282	3.45
4 mm	1.408	62.94	1.837	38.94	4.718	58.02	5.652	36.56

Table V
Numerical simulation ratio results for UG2 reef

Cutting depth	FN'/FN	% Error	FD'/FD	% Error	F/FD	% Error
2 mm	2.96	5.82	2.96	3.55	1.016	18.75
4 mm	3.35	13.2	3.07	3.95	0.766	39.17

The results in the tables show that the model parameters can be updated through trial and error to give similar results as the experimental results. But this only works when updating the model parameters so that the numerical simulation results are similar to the results for one particular set of experimental cutting parameters, in this case, a cutting depth of 2 mm. For the 2 mm cutting depth the percentage error for the force values is acceptable when compared to the percentage error in table Table III. Thus, the numerical simulation set-up can be updated so that acceptable results are obtained. When using the same model set-up for a cutting depth of 4 mm, as used for the 2 mm cutting depth, the results are less than ideal as indicated by the percentage errors shown in table Table IV.

This inability to generate the model parameters to be applicable to a large range of cutting parameters has also been observed by other researchers in previous work (Huang, et al., 2016; Jaime, et al., 2015). It was assumed that the error when changing cutting depth was due to poor modelling of the cutting tool. However, after the results of the numerical simulations were obtained it is clear that the error is due to other factors.

The results in Table V show that the ratios of peak force to mean force for both the normal force and the drag force, are close to 3, which is the same as the experimental results. This ratio was obtained by changing the element size. The material properties were updated so that the peak forces are similar, after which the element size was edited to get the correct ratio. The peak force to mean force ratio is acceptable for both cutting depths. Lastly, this study considers the ratio of the mean normal force to the mean drag force. Previous researchers also experienced a difficulty to get this ratio correct (Huang, et al., 2016; Su and Akcin, 2011; Van Wyk, et al., 2014). The contact parameters are important factors that change the ratio as well as element size. This ratio does not have an acceptable accuracy.

This section showed that it is possible to use Ansys LS-DYNA with the CSCM to model rock cutting of UG2 reef samples and get acceptable results, but the user must calibrate the model parameters using the experimental results. Thus, the model is only fit for one set of cutting parameters. The section showed that the model does not extrapolate accurately when the cutting parameters are changed.

Conclusion

Rock cutting using conical picks is a common method of mining that enables continuous mining operations. Various research projects have been conducted on different design aspects using conical picks. None of these studies considered rock samples found in South African hard rock environments, such as the UG2 reef samples.

The main observation when cutting UG2 reef sample, is that it has large variance in strength on a millimeter scale. This introduces uncertainty in the results due to added variance from one cutting experiment to another for the same UG2 reef sample. Another problem is the inconsistency in rock properties of the UG2 reef, when examining the rock properties from one mine to another.

The results indicated that the optimal s/d ratio for the different cutting parameters follow the expected trends. But the normal force, drag force, and specific energy plateaus at a cutting depth of 4 mm for larger s/d values when cutting UG2. This implies that the depth of cut has a larger influence on the cutting force results of UG2 reef samples. Clearly, using optimized cutting parameters form cutting test performed on other material than UG2 might not be appropriate to use to make design decisions for mining equipment intended for UG2.

At 2 mm cutting depth the force signals were impulsive, and the material collected was of fine fragmentation. At a cutting depth of 4 mm the force signals had a saw tooth shape. This implies that larger chips are formed. However, the UG2 produced fine fragmentation. This is undesirable in underground mining conditions owing to the difficulty of cleaning this fine fragmentations from the stopes.

Using the fast Fourier transform (FFT) analysis is a useful method to discuss and compare rock cutting data. Valuable information can be obtained when looking at the FFT analysis, such as if the cutting force signal is periodic and the size of the fragmentation. This was true for material with little to no variance in strength on a millimeter scale, such as sandstone. The results for the UG2 however showed that the conclusions are not clear. Owing to the UG2 not being periodic, because of the UG2 having large variance in strength on a millimeter scale, the FFT analysis did, in this case, not give useful information about the size of the fragmentation.

The numerical simulations illustrated that there are various model parameters that influence the results and some that do not influence the results. Some parameters are based on material properties and other are updated through trial and error. The parameters are updated by changing model parameters and the material properties used in the equations given by (Novozhilov, et al., 2022), until an acceptable accuracy is obtained between the numerical simulation cutting results and the experimental cutting results for a constant set of cutting parameters.

It is possible to model rock cutting of UG2 reef samples using LS-DYNA and the CSCM. But this is only possible by updating the model parameters through trial and error for one set of cutting parameters. When the cutting parameters are changed, such as the cutting depth, the model does not produce acceptable results. Thus, the model is not capable of extrapolation.

In conclusion, it is unclear at this stage if conical picks can be used for mechanized mining in the UG2 hard rock environment, as the fine fragmentation will make the mining process impossible. This observation is based on a laboratory scale cutting test conducted on actual rock samples and further work is clearly necessary.

It was also shown that it is possible to simulate the cutting process using FEM software. Previous researchers have also successfully used FEM to simulate rock cutting, but not for rock found in deep hard rock environments in South Africa. The model, however, does not produce good results when extrapolating beyond the specific conditions considered to obtain the rock characteristics, for example, for different cut depths. Further research will be required to address the generalization of modelling.

Acknowledgements

The authors gratefully acknowledge the support that was received from the Mandela Mining Precinct through their SAMERDI programme.

References

Bilgin, N., Copur, and H., Balci, C. 2013. *Mechanical excavation in mining and civil industries*. Boca Raton: CRC Press.

Copur, H., Bilgin, N., Balci, C., Tumac, D. Avunduk, E. Effects of different cutting patterns and experimental conditions on the performance of a conical drag tool. *Rock Mechanics and Rock Engineering*, vol. 50, no. 6, pp. 1585–1609.

Dehkhoda, S., Detournay, E. 2019. Rock cutting experiments with an actuated disc. *Rock Mechanics and Rock Engineering*, vol. 52, no. 9, pp. 3443–3458.

Evans, I. 1962. A theory of the basic mechanics of coal ploughing.. *Proceedings of the International Symposium on Mining Research*, vol. 2, no. 1, pp. 761–768.

Goktan, R., Goktan, H.G., Goktan, M.H. 1997. A suggested improvement on Evans cutting theory for conical bits.. *Proceedings of the fourth international symposium on mine mechanization and automation*, vol. 1, no. 1, pp. 57–61.

Hekimoglu, O.Z. 2018. Investigations into tilt angles and order of cutting sequences for cutting head design of roadheaders. *Tunnelling and Underground Space Technology*, vol. 76, pp. 160–171.

Höll, H. 2009. *Pillar design and cutting at Everest platinum mine*, South Africa: Aquarius Platinum (South Africa) (Pty) Ltd..

Huang, J., Zhang, Y., Zhu, L., Wang, T. 2016. Numerical simulation of rock cutting in deep mining conditions. *International Journal of Rock Mechanics and Mining Sciences*, vol. 84, pp. 80–86.

Jaime, M.C. 2011. *Numerical modeling of rock cutting and its associated fragmentation process using the finite element method*, s.l.: University of Pittsburgh Swanson School of Engineering.

Jaime, M.C., Zhou, Y., Lin, J.-S. and Gamw, I.K. 2015. *Finite element modeling of rock cutting and its fragmentation process*, Pittsburgh, PA, USA: Department of Civil and Environmental Engineering, University of Pittsburgh.

Kalogeropoulos, A., Michalakopoulos, T. 2021. *Numerical simulation of rock cutting using YADE*. s.l., s.n.

Kang, H., Cho, J.-W., Park, J.-Y., Jang, J.-S., Kim, J.-H., Kim, K.-W., Rostami, J., Lee,J.-W. A new linear cutting machine for assessing the rock-cutting performance of a pick cutter. *International Journal of Rock Mechanics and Mining Sciences*, vol. 88, pp. 129–136.

Li, B., Zhang, B., Hu, M., Liu, B., Cao, W. Xu, B. 2022. Full-scale linear cutting tests to study the influence of pre-groove depth on rock-cutting performance by {TBM} disc cutter. *Tunnelling and Underground Space Technology incorporating Trenchless Technology Research*, vol. 122, no. 104366.

Livermore Software Technology (LST), an ANSYS company, 2021. *LS-DYNA Keyword user's manual volume III*. Livermore, California: Livermore Software Technology.

Mendyka, P. 2017. *Laboratory stand tests of mining asymmetrical disc tools.* s.l., s.n.

Moxham, K. 2004. *A narrow reef mining machine - ARM1100*. s.l., The South African Institute of Mining and Metallurgy, pp. 207–214.

Novozhilov, Y.V., Dmitriev, A.N., Mikhaluk, D.S. 2022. *Precise calibration of the continuous surface cap model for concrete simulation*., s.l.: Buildings.

Park, J.Y., Kang, H., Lee, J.-W., Kim, J.-H., Oh, J.-Y., Cho, J.-W., Rostami, J., Kim, H.D. 2018. A study on rock cutting efficiency and structural stability of a point attack pick cutter by lab-scale linear cutting machine testing and finite element analysis. *International Journal of Rock Mechanics and Mining Sciences*, vol. 103, no. 13651609, pp. 215–229.

Pickering, R.G.B. 2007. Has the South African narrow reef mining industry learnt how to change?. *The Journal of The Southern African Institute of Mining and Metallurgy*, vol. 107, pp. 557–565.

Stopka, G. 2021. Modelling of rock cutting with asymmetrical disc tool using discrete-element method (DEM). *Rock Mechanics and Rock Engineering*, vol. 54, no. 12, pp. 6265–6279.

Su, O., Akcin, N.A. 2011. Numerical simulation of rock cutting using the discrete element method. *International Journal of Rock Mechanics and Mining Sciences*, vol 48, no. 3, pp. 434–442.

Van Wyk, G., Els, D.N.J., Akdogan, G., Bradshaw, S.M., Sacks, N. 2014. Discrete element simulation of tribological interactions in rock cutting. *International Journal of Rock Mechanics and Mining Sciences*, vol. 65, pp. 8–19.

Vogt, D. 2016. A review of rock cutting for underground mining: Past, present, and future. *South African Institute of Mining and Metallurgy*, vol. 116, no. 11, pp. 1011–1026.

Wicaksana, Y., Jeong, H., Jeon, S. 2021. Numerical simulation of rock cutting process induced by a pick cutter considering dynamic properties of rock at intermediate strain rate. *Bulletin of Engineering Geology and the Environment*, vol. 80, no. 12, pp. 9049–9069.

Zárate, F., Oñate, E. 2015. A simple FEM–DEM technique for fracture prediction in materials and structures. *Computational Particle Mechanics*, vol. 2, no. 3, pp. 301–314.

Zou, J., Yang, W.,h Han, J. 2020. Discrete element modeling of the effects of cutting parameters and rock properties on rock fragmentation. IEEE Access, vol. 8, pp. 136393–136408. ◆